Modelling Wind Velocity Patterns for Windbreak Fence Design

Se-Woon Hong, Division M3-BIORES: Measure, Model & Manage Bioresponses, KU Leuven, Kasteelpark Arenberg 30, B-3001 Leuven, Belgium

In-Bok Lee and Hyun-Seob Hwang, Seoul National University, 599 Gwanangno Gwanakgu, Seoul, Republic of Korea

Abstract

The use of windbreak fences has become a common practice to reduce wind erosion and soil particle dispersion in potentially risky areas, such as reclaimed lands, harvested fields and sandy beaches. However, the windbreak design in terms of screen porosity, fence height and distance between multiple fences is still determined by empirical knowledge. For the effective and economical use of windbreak fences, this paper introduces a regression model to predict wind speed reduction by windbreak fence according to screen porosity, fence height, fence location and wind speed. The regression model is able to predict the effects of single fence as well as multiple fence array and to provide straightforward procedures for windbreak fence design. The model was developed by non-linear regression analysis based on the data obtained from computational fluid dynamics (CFD) simulations, which was validated in advance by wind tunnel experiments. The porous characteristics of the screen were accurately measured by a small wind tunnel in the forms of the inertial resistance (C_{ir}) and permeability (α) of Darcy-Forchheimer law for specifying porous media. The regression coefficients were estimated by a genetic algorithm. The regression model for single fence showed good agreement to the simulation results with R^2 = 0.997 and 0.999 at leeward and windward, respectively. The model for multiple fences were derived from multiplication of the model for single fence and also showed a good agreement with the simulation results. The regression models for single and multiple fences provided handy charts and a program for users to easily design a windbreak fence or fence array.

Keywords: percent of upcoming velocity (PUV), porous fence, non-linear regression, computational fluid dynamics (CFD)

1 Introduction

Windbreaks have been used for many years as a wind erosion control measure against losses of valuable loam and nutrients in agricultural land and dispersion of eroded particles and dust to nearby habitation (Hong et al., 2014). They have been mostly used in the form of natural vegetative barriers against wind (Comelis and Gabriels, 2005). However, designing vegetative barriers can be difficult because the characteristics of vegetation, such as rigidity, leafiness, leaf and stem shape and density distribution, cannot be easily controlled (Bilbro and Stout, 1999) and are not homogeneously distributed and even change with time. Therefore, non-vegetative barriers, mostly porous fences, have also been studied to provide more rapid and reliable shelter effects (Grantz et al., 1998). The porous fences, generally windscreen fences or windbreak fences, have been studied for the many purposes, such as reduction of wind-blown particle emission in open coal yards (Cong et al., 2011) and reduction

of dust generation and diffusion from a huge reclaimed land (Bitog et al., 2009). However most of the studies were conducted to a specific problem and provide limited information on the various uses of windbreak fences.

The objective of this study was to develop a prediction equation to describe wind speed reductions by windbreak fences in order to provide efficient design suggestions. The three main parameters for the windbreak fence design were fence porosity, fence height and wind speed, and the prediction equation calculated vertical and horizontal percent of upcoming velocity (PUV) distributions based on the results of commercial computational fluid dynamics (CFD) simulations. For reliable CFD simulations, wind tunnel experiments were conducted in advance and used to validate the simulation. The equations presented in this study will be available to predict wind speed reductions by various arrays of multiple fences in terms of their spacing and fence porosities for design purposes.

2   Materials and methods

The study was conducted by three parts: CFD model validation, data generation and regression. During the CFD model validation part, wind tunnel test were conducted to collect wind speed data measured at windward and leeward of the windbreak fence. The porosity of the fence screen was measured in terms of the pressure loss coefficient for modelling purposes. For data generation, CFD simulation models were designed and validated using measured data. The vertical and horizontal distributions of PUV were calculated according to the fence porosity, fence height, wind speed and fence array. Much of PUV data produced by the simulation was processed to obtain equations to describe the windbreak effect of single and multiple fences by non-linear regression analysis. For the CFD simulation, the commercial CFD packages FLUENT (ver. 6.3, Fluent Inc., NH, USA) and GAMBIT (ver. 2.4, Fluent Inc., NH, USA) were used.

2.1   Tested fence screen

The fence screen used in this study consisted of a commercially available screen that had a mesh size of 3 mm x 9 mm. Since it has been used as a single layer or as multiple layers, the pressure los coefficient of the screen was investigated according to the number of layers. The pressure loss coefficient of the screen was measured by a pressure-drop measurement system that consisted of a small wind tunnel and a digital micro-manometer (TSI 5815, TSI Inc., USA) with three pitot tubes (Kim et al., 2013) as shown in Figure 1. The tested screens were mounted at the pipe between two pitot tubes and the pressure loss by screens was calculated by the pressure difference between two pitot tubes and using equation (1) based on the Bernoulli's principle.
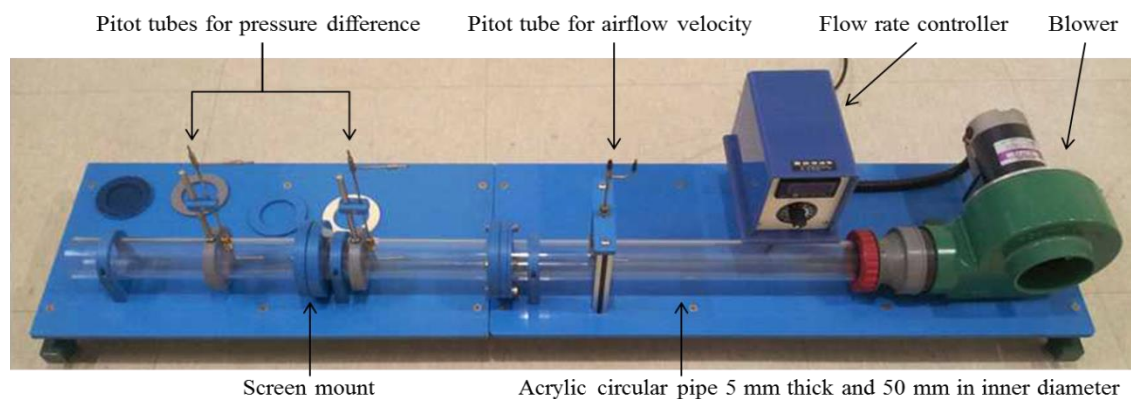

Figure 1: Pressure-drop measurement system to measure the pressure loss coefficient of screens

$$\Delta p_s = (p_2 - p_1) - \rho g \left(f \frac{L}{D} \frac{u^2}{2g} \right) \qquad (1)$$

Δp_s is the pressure loss caused by the screens (kg m^{-1} s^{-2}), p_2 and p_1 are the pressures measured at two pitot tubes (kg m^{-1} s^{-2}), ρ is the fluid density (kg m^{-3}), g is the gravitational acceleration (m s^{-2}), f is the friction coefficient of the acrylic pipe, L is the length between two pitot tubes (m), D is the pipe diameter (m), and u is the fluid velocity in the pipe (m s^{-1}).

The measured pressure losses were expressed by a quadratic equation with respect to the fluid velocity which corresponds to the Darcy-Forchheimer equation shown in equation (2). The pressure loss coefficient and viscous resistance coefficient of screens were calculated by the least square method. Because in practice the screen is used in a multi-layered form to increase windbreak effects, the pressure losses by two-layered and three-layered screens were also tested.

$$\Delta p_s = -\left(\frac{\mu}{\alpha}u + C_{ir}\frac{1}{2}\rho u^2\right) \qquad (2)$$

α is the viscous resistance coefficient or permeability of screens (m^{-1}), and C_{ir} is pressure loss coefficient or inertial resistance coefficient of screens.

2.2 Wind tunnel experiment and CFD modelling validation

Tested screen was installed in a wind tunnel located at the National Institute of Agricultural Engineering (NIAE), Korea. The wind tunnel test section had the dimensions of 2 m (W) x 1.7 m (H) x 15 m (L), and the fence height was 0.2 m considering the small blockage ratio, which is the ratio of the model area relative to the cross sectional area of the wind tunnel. A total of six cases were tested with three sets of screens (1 layer, 2-layered and 3-layered) and two wind speeds (2 m s^{-1} and 4 m s^{-1}). The wind speed reduction by the fence was measured at leeward distances of 0.1, 0.2, 0.3, 0.4, 0.5, 0.6, 0.8 and 1.0 m behind the fence and at a height of 0.1 m above the floor.
CFD model of the same configuration with the wind tunnel experiment was validated by evaluating whether it predicted wind speed reduction by porous fences well. The validation points were the appropriate mesh size and turbulence model and whether a two-dimensional model produced reasonable results compared to a three-dimensional model because if possible two-dimensional model can effectively reduce computational time and cost.

2.3 Data generation

The validated simulation method were applied to CFD models for predicting wind speed reductions by single fences considering 54 cases with three fence heights (1.1, 1.5 and 2.0 m), three screens (1 layer, 2-layered and 3-layered), and six wind speeds at the height of the fence top (5, 8, 11, 14, 17 and 20 m s-1). For double fences, 36 cases were studied, with two wind speeds (8 and 17 m s^{-1}), three screens (1 layer, 2-layered and 3-layered), and six fence spacings (5H, 10H, 15H, 20H, 30H and 40H, where H is the fence height.). For triple fences, two cases with two wind speeds (8 and 17 m s^{-1}) were examined. The size of the entire computational domain was 40 m and 80 m in the windward and leeward directions respectively, from the fences and 11 m above the fences. The fences were set as the wall boundary condition with a porous jump condition (Fluent, 2007). The porous jump condition enables pressure drops by a porous medium as expressed by equation (2). The simulations were carried out in Fluent with a steady state solver. The vertical profiles of wind speed, turbulence quantities at the inlet boundary and the momentum sink designed by Hong et al. (2011) were applied to the models.
The simulated wind speed reductions were expressed by PUV. The PUV has been calculated at one height, but in this study, the PUV was defined as the average of PUVs at heights of between the ground and the fence top. For easier calculation we defined the vertically averaged velocity (VAV) and the PUV can be calculated as the ratio of the VAV with the fence to the VAV without the fence.

2.4 Regression process

PUVs with respect to the downwind distance behind the fence showed complex curves but could be expressed as the sum of two exponential terms as shown in equation (3).

$$PUV(x) = a \exp\left(-b\frac{x}{H}\right) - c \exp\left(-d\frac{x}{H}\right) + e \tag{3}$$

x is the horizontal position or distance from the fence (m), and a, b, c, d and e are the regression coefficients.

We assumed that the effects of layers, fence heights and wind speeds on the PUV distribution were included in the regression coefficients and defined the regression coefficients as a function of them. This assumption again generated many regression coefficients. Therefore, a genetic algorithm was used to search for optimal values for the regression coefficients in MATLAB (ver. 2010a, MAthWorks). In this study, the MATLAB code for the continuous genetic algorithm provided by Haupt and Haupt (2004) was used.

3 Results and discussion

To calculate pressure loss coefficient and viscous resistance coefficient of the tested screens, the pressure loss by screens according to various fluid velocities were measured and displayed in Figure 2. The quadratic polynomials showed good agreement with the measured data in all test cases, and therefore, the calculated coefficients were considered reliable. In Figure 2, a linear relationship was found between the coefficients and the number of layers. For the pressure loss coefficient, the relationship was expressed as $C_{ir} = 0.8529\,N$ with R^2=0.999, where N is the number of layers. There was also a good agreement (R^2=0.999) between the viscous resistance coefficient and the number of layers, expressed as $1/\alpha = 0.3466\,N$ ($\times 10^5$).
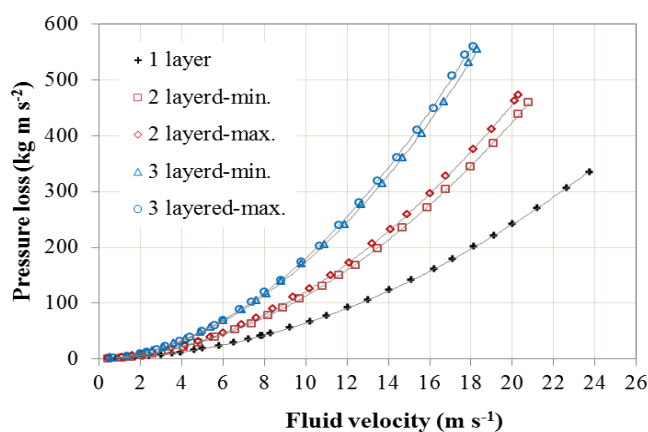

Figure 2: The measured pressure losses by screens with respect to the fluid velocity. The lines indicate the regression curves in the forms of a quadratic polynomial.

For the CFD modelling validation, the simulated wind reduction were compared to wind tunnel experimental results as shown in Figure 3. As results of validation test, the simulated wind speeds were not significantly affected by the turbulence model at the distance of 0 to 1.2 m, but however, the RNG k-ε model showed the lowest error. The mesh size did not have much influence on the simulated wind speeds either. The relative errors between the simulated and measured results at the distance of 0 to 1.2 m were 2.5, 2.67, 3.01, 3.47 and 3.73 % for mesh sizes of 0.015, 0.02, 0.03, 0.04 and 0.08 m respectively. The appropriate mesh size was determined to be 0.04 m considering computational cost and time. The 2D simpli-

fied model with a mesh size of 0.04 m using the RNG k-ε turbulence model was also tested and compared to the results of the 3D models. The relative errors of leeward wind speeds between 2D and 3D models were 1.13, 1.70 and 2.19 % for 1 layer, 2-layered and 3-layered respectively, proving the 2D model was suitable for the simulation of windbreak fences.
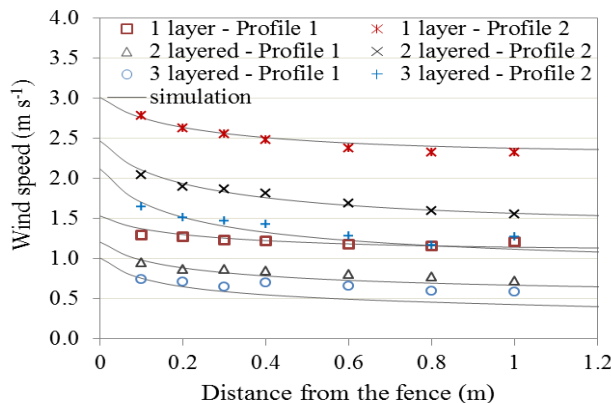

Figure 3: Wind speeds with respect to distance behind the fence measured by wind tunnel experiments and calculated by CFD simulations.

Data generation was conducted by the 2D simulations and the simulated results are shown in Figure 4 which shows the PUV distributions according to fence heights and wind velocities. From Figure 4 we found three interesting points. One is that the PUV curves of the three fence heights are almost identical if the horizontal axis is converted into non-dimensional space, which means that the effect of fence height on PUV distribution can be simply estimated by the geometrical similarity of the PUV curves. As long as the wind speed at the fence top is identical, simulations of different fence heights have an identical fence Reynolds number, and theoretically they are geometrically-similar to each other. The second is that the fence porosity affected the maximum PUV reductions rather than the windbreak distances. As the fence porosity decreased, the maximum PUV reduction markedly increased but the increased was not linear and expected to be converged at a certain porosity level. The third is that the wind speed increased the windbreak effect was extended farther. Such an extension of the windbreak effect was shown to decreased as wind speed increased and is expected to be infinitesimal at a certain high wind speed.
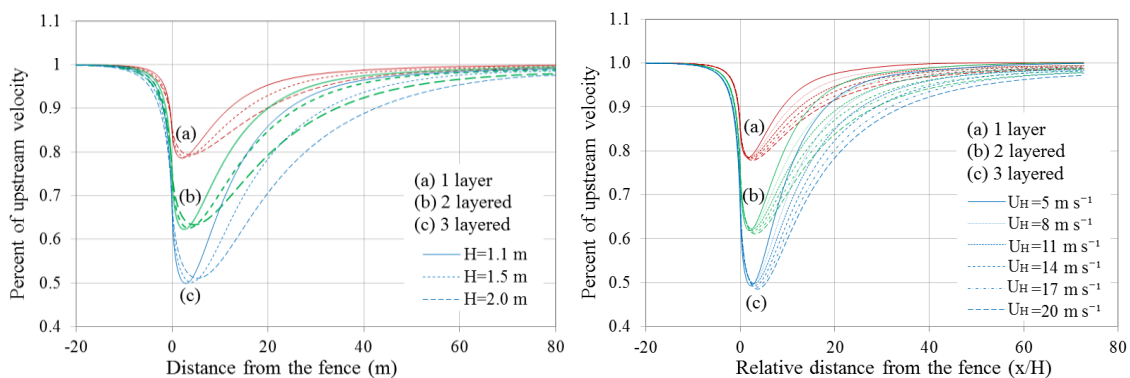

Figure 4: Simulated PUV distributions according to fence heights (left) and wind speeds (right) at the fence top.

The curves of PUVs with respect to the relative distance behind the fence can be expressed as the sum of two exponential terms in equation (3) as previously stated. Here the coefficient e becomes one mathematically because the PUV become one at a certain long distance. The other four coefficients were estimated by a genetic algorithm using the PUV data of six wind speeds and three screen layers. According to the estimation, the four regression coefficients were affected by the fence porosity and wind speed. Therefore we could presume that the four regression coefficients were expressed as sub-regression equations, i.e. the sum or

product of of N or N^c and $U_H{}^c$ or $\ln(U_H)$, where N is the number of screen layers, U_H is the wind speed at the height of fence top, and c is a constant. Accordingly, sub-equations that could be used to estimate the regression coefficients were assumed in the following 8 forms: a or b or c or d = (1) $c_1 N \times U_H{}^{c_2} + c_3$, (2) $c_1 N \times \ln(U_H) + c_2$, (3) $c_1 N + c_2 U_H{}^{c_3} + c_4$, (4) $c_1 N + c_2 \ln(U_H) + c_3$, (5) $c_1 N^{c_2} \times U_H{}^{c_3} + c_4$, (6) $c_1 N^{c_2} + c_3 U_H{}^{c_4} + c_5$, (7) $c_1 N^{c_2} + c_3 \ln(U_H) + c_4$, (8) $c_1 N^{c_2} \times \ln(U_H) + c_3$.

The appropriate sub-equations and their regression coefficients of the sub-equations were also estimated by a genetic algorithm. Skipping the details on the regression processes, the simulated PUVs and those calculated by equations (4) ~ (7) finally showed good agreement, with R^2 = 0.997 for six wind speeds and three screen layers.

$$a = c_1 N + c_2 U_H{}^{c_3} + c_4 \qquad (4)$$
$$b = c_5 N^{c_6} + c_7 \ln(U_H) + c_8 \qquad (5)$$
$$c = c_9 N + c_{10} U_H{}^{c_{11}} + c_{12} \qquad (6)$$
$$d = c_{13} N^{c_{14}} \times U_H{}^{c_{15}} + c_{16} \qquad (7)$$

N is the number of screen layers, and U_H is the wind speed at the height of fence top.

In the same way, the PUVs at the windward side of the fence (x<0) could be expressed as a simple exponential curve as shown in equation (8).

$$PUV(x) = 1 - (c - a)exp\left(-c_{17}\left(-\frac{x}{H}\right)^{c_{18}}\right) \qquad \text{for } x \leq 0 \qquad (8)$$

The optimal values of the regression coefficients were found in Table 1.

Table 1: Regression coefficients for sub-equations (15) ~ (18)

Coefficient	c_1	c_2	c_3	c_4	c_5	c_6	c_7	c_8
Value	0.1249	0.8472	-1.6366	-0.0027	0.5198	-0.4480	-0.0799	0.4010
Coefficient	c_9	c_{10}	c_{11}	c_{12}	c_{13}	c_{14}	c_{15}	c_{16}
Value	0.2228	1.6746	-1.9539	0.0644	0.4166	-0.1629	-0.9370	0.0393

For double or multiple fences, the simulation results showed that the simulated PUV curves by multiple fences were more like the product of individual PUVs rather than their superposition. This is physically reasonable because the wind speeds reduced by the first fence become the incoming wind speeds from the point of view of the second fence. Finally, the product of multiple individual PUVs is presented in Figure 5 and Figure 6 as 'Equations' and showed good agreement with the simulated PUV distributions in all cases.

The PUV distribution of double or triple fences was calculated by equations (9) and (10), which can be used to predict PUV distributions by multiple fences.

$$PUV^{(k)}(x) = \prod_{j=1}^{k} PUV_{fence\ j}(x) = \prod_{j=1}^{k} PUV\big(N_j,\ V_{j-1}(d_j),\ x - d_j\big) \qquad (9)$$

$PUV^{(k)}(x)$ is the PUV distribution with respect to the horizontal position x produced by k fences, k is the number of fences, $PUV_{fence\ j}$ is the PUV distribution produced by the individual j-th fence, N_j is the number of screen layers of the j-th fence, $V_{j-1}(x)$ is the VAV at the position of x produced by $(j-1)$ fences (m s^{-1}), i.e., from first fence to $(j-1)$-th fence, and d_j is the horizontal position of the j-th fence (m).

The term $V_{j-1}(d_j)$ can be formulated as equation (10) by its definition.

$$V_{j-1}(d_j) = V_0 \times PUV_{fence\ j-1}(d_j) \qquad (10)$$

V_0 is the VAV of the initial or upstream wind profile (m s^{-1}).

The PUV prediction for multiple fences is accompanied by the product of a sequence of terms and requires a number of calculations. However, the equations are simple and repetitive and thus can be solved by a simple programming.
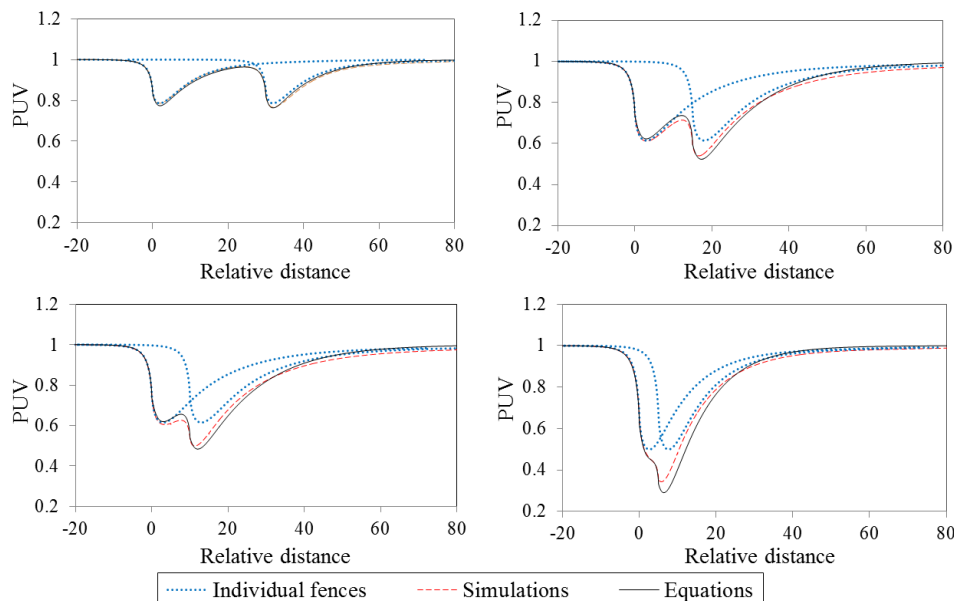

Figure 5: Comparisons of PUV distribution by double fences simulated by CFD models and calculated from the PUVs of individual fences.
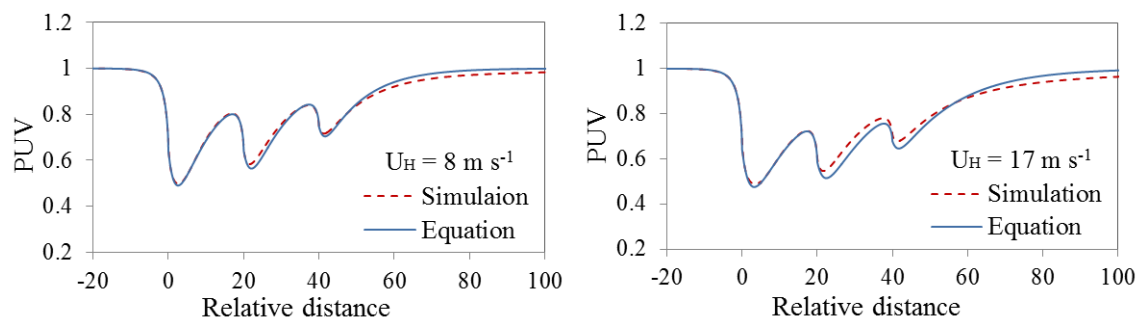

Figure 6: Comparisons of PUV distributions by triple fences simulated by CFD simulation models and calculated by equations of this study. Three fences with 3, 2 and 1 layers were located at the position of 0, 20 and 40, respectively.

4   Conclusions

The predictive equations to describe wind speed reductions by windbreak fences were developed in this study by non-linear regression analysis based on data obtained from CFD simulations. For design purposes, the developed prediction equations provide a straightforward procedure to predict the windbreak performance of a single as well as multiple fences. Even though this research still needs to be improved by in situ validation and the development of more applicability, the results of this study can be a good starting point for designing windbreak fences in many areas, such as for agricultural and industrial uses, because they provide immediate understanding of the wind speed reduction according to various design factors.

5   Acknowledgements

6   References

Bilbro, J.D., & Stout, J.E. (1999). Wind velocity patterns as modified by plastic pipe windbarriers. *Journal of Soil and Water Conservation, 54(3)*, 551-556.

Bitog, J.P., Lee, I.-B., Shin, M.-H., Hong, S.-W., Hwang, H.-S., Seo, I.-H., Yoo, J.-I., Kwon, K.-S., Kim, Y.-H., & Han, J.-W. (2009). Numerical simulation of an array of fences in Saemangeum reclaimed land. *Atmospheric Environment, 43*, 4612-4621.

Cong, X.C., Cao, S.Q., Chen, Z.L., Peng, S.T., & Yang, S.L. (2011). Impact of the installation scenario of porous fences on wind-blown particle emission in open coal yards. *Atmospheric Environment, 45*, 5247-5253.

Cornelis, W.M., & Gabriels, D. (2005). Optimal windbreak design for wind-erosion control. *Journal of Arid Environments, 61*, 315-332

Fluent (2007). *Fluent documentation*. Fluent Inc., Lebanon, NH.

Grantz, D.A., Vaughn, D.L., Farber, R.J., Kim, B., VanCuren, T., & Campbell, R. (1998). Wind barriers offer short-term solution to fugitive dust. *California Agriculture, 52(4)*, 14-18.

Haupt, R.L., & Haupt, S.E. (2004). *Practical genetic algorithms, second edition*. Wiley-Interscience, New Jersey, USA, 215-219.

Hong, S.-W., Lee, I.-B., Seo, I.-H., Kwon, K.-S., Kim, T.-W., Son, Y.-H., & Kim, M. (2014). Measurement and prediction of soil erosion in dry field using portable wind erosion tunnel. *Biosystems Engineering, 118*, 68-82.

Kim, R.-W., Lee, I.-B., Hong, S.-W., Hwang, H.-S., Son, Y.-H., Kim, T.-W., Kim, M.-Y., & Song, I. (2013). Measurement of aerodynamic properties of screens for windbreak fence using the apparatus of testing screens. *Journal of the Korean Society of Agricultural Engineers, 55(6)*, 145-154. (In Korean)